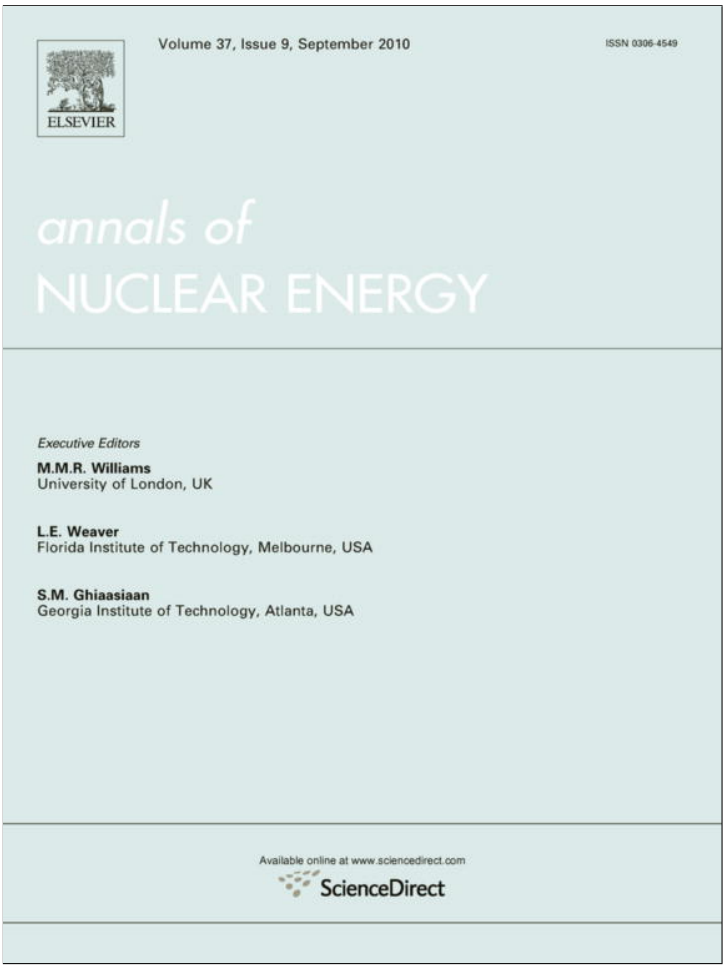

Annals of Nuclear Energy 37 (2010) 1139–1145

Contents lists available at ScienceDirect

Annals of Nuclear Energy

journal homepage: www.elsevier.com/locate/anucene

Validation of the Monte Carlo model supporting core conversion of the Portuguese Research Reactor (RPI) for neutron fluence rate determinations

A.C. Fernandes [a,b,*], J.P. Santos [a], J.G. Marques [a,b], A. Kling [a,b], A.R. Ramos [a,b], N.P. Barradas [a,b]

[a] Instituto Tecnológico e Nuclear, Estrada Nacional 10, P-2686-953 Sacavém, Portugal
[b] Centro de Física Nuclear da Universidade de Lisboa, Av. Prof. Gama Pinto, 2, P-1649-003 Lisboa, Portugal

ARTICLE INFO

Article history:
Received 9 February 2010
Received in revised form 5 May 2010
Accepted 6 May 2010
Available online 31 May 2010

Keywords:
Reactor modelling
Monte Carlo simulation
Neutron fluence rate measurement
Activation method

ABSTRACT

The Monte Carlo code MCNP was used to calculate absolute values of thermal, epithermal and fast neutron fluence rates in the new RPI core using fresh LEU fuel. Discrepancies smaller than 20% were obtained between calculated results and activation foil measurements. A previous knowledge of general characteristics of the neutron energy spectra, provided by the MCNP reactor model itself, has been fundamental to determine the conditions yielding a proper comparison of simulated and measured results. An excellent agreement (6%) was also obtained for the relative neutron fluence rate profiles along the fuel height. The MCNP model of the reactor core was therefore validated for a tri-dimensional determination of neutron fluence rates in the fuel assemblies and neighbouring irradiation positions.

1. Introduction

The RPI is a 1 MW pool-type reactor built by AMF Atomics (USA) and commissioned in 1961. Core conversion to low-enriched uranium (LEU) was concluded in 2007, after a feasibility study made with the assistance of the Reduced Enrichment for Research and Test Reactors (RERTR) program, in which the Monte Carlo code MCNP-4C (Briesmeister, 2000) was used for core analysis via neutronics calculations (Matos et al., 2006).

MCNP simulations of the RPI were performed in past for the former HEU core, integrating fuel with burnup as high as 25% (Fernandes et al., 2003). In these investigations, a two-dimensional deterministic model with reduced energy and space discrimination was used to estimate the fuel burnup and describe its composition as a function of burnup (Barradas et al., 2000). The MCNP model was a major improvement towards the description of neutron spectra in the reactor core and neutron beams (Fernandes et al., 2006). Nevertheless important discrepancies were observed between calculated and measured multiplication factors, scaled neutron fluence rates for a specific reactor power and neutron fluence rate profiles along the fuel height. For this reason, the core model reliability was limited to the determination of relative neutron fluence rates in the horizontal plane and energy spectra, to be scaled afterwards through comparison with an experimental result. The poorly accounted fuel burnup and composition were suggested as an explanation for these limitations.

In the present work, the MCNP model developed for the new LEU core of the RPI is compared with neutron fluence rate measurements performed shortly after the reactor commissioning, when fresh fuel conditions can be assumed. This study allows an evaluation of the model for the determination of absolute neutron fluence rates and vertical neutron fluence rate profiles, in favourable conditions to be considered for future reference in the analysis of effects such as fuel burnup and cross section libraries in the model's accuracy.

2. Materials and methods

2.1. Core configuration

The investigated core configuration (Fig. 1) consists of seven standard and five control fuel assemblies manufactured by AREVA CERCA (France), with approximate dimensions of $(8 \times 8 \times 60)$ cm.

The core is reflected by a graphite thermal column, beryllium and light water. Four dummy assemblies were introduced in order to improve the thermal hydraulic safety margin. The fuel, dummies and beryllium reflectors are mounted on a grid plate with a 9×6 pattern. Samples are routinely irradiated in the free grid positions, in the dummies and in cavities at some beryllium reflectors. The dummies consist of the same external structure as fuel assemblies but contain instead of fuel plates only an aluminium tube in the central region allowing sample irradiation.

* Corresponding author at: Instituto Tecnológico e Nuclear – Unit of Reactors and Nuclear Safety, Estrada Nacional 10, P-2686-953 Sacavém, Portugal. Tel.: +351 219 946 152; fax: +351 219 941 039.
E-mail address: anafer@itn.pt (A.C. Fernandes).

0306-4549/$ - see front matter © 2010 Elsevier Ltd. All rights reserved.
doi:10.1016/j.anucene.2010.05.004

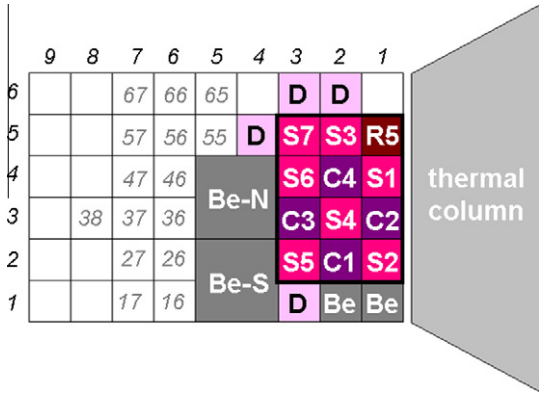

Fig. 1. The N2-P1/2 configuration of the RPI core. (Be: beryllium reflector; C: control fuel assembly hosting a control rod; D: dummy assembly; S: standard fuel assembly; R: control fuel assembly hosting a regulating rod). The free grid positions where measurements were made are identified in italic.

The fuel is of Material Test Reactor (MTR) type, in the shape of flat plates using uranium silicide (U_3Si_2–Al) alloy with nominally 19.75% enriched uranium. Control and standard fuel assemblies (Fig. 2) contain 10 and 18 fuel plates, respectively, with approximately 20.9 g of ^{235}U per plate. For identification throughout the text, the 3 mm-thick water channels between fuel plates are numbered along the pool-to-thermal column direction.

There are four safety rods and one regulation rod located in the control assemblies. The safety rod consists of a 1 mm-thick cadmium foil supported and covered by 1.5 mm-thick stainless steel, while the regulating rod is a hollow 2.2 mm-thick stainless steel tube. Rods have oval cross-sectional shapes and 61 cm length. When fully inserted, rods centreline is displaced 14 mm above that of the fuel meat.

Further details about the fuel description and assemblies design are given in Table 1 and reported in Matos et al. (2006).

2.2. Measurements

2.2.1. Irradiation positions

Neutron fluence rates were measured in the water channel No. 5 of standard fuel assemblies S3, S5, S6 and S7, in all dummies, in the beryllium reflector Be–N, and in the free grid positions identified in Fig. 1.

Table 1
Summary of RPI core design data.

Fuel type	MTR plate
Meat composition	U_3Si_2–Al
Nominal enrichment in ^{235}U (%)	19.75
Average mass of ^{235}U per plate (g)	20.9
Cladding material	AG3NE alloy
Number of plates per assembly	Standard: 18; Control: 10
Number of assemblies (initial core)	Standard: 7; Control: 5
Meat dimensions (mm)	$0.6 \times 63.4 \times 596.9$
Plate dimensions (mm)	$1.37 \times 71.0 \times 625.5$
Assembly dimensions (mm)	$79.8 \times 75.9 \times 714.4$
Cladding thickness of fuel plate (mm)	0.38
Coolant channel thickness (mm)	3.05
Absorber material in control rod	Cd
Absorber material in regulating rod	Stainless steel 18/10
Cladding material of control rod	Stainless steel 18/10
Number of rods	Control: 4; Regulating: 1
External dimensions of control rod (mm)	$56.0 \times 21.0 \times 642.0$
External dimensions of regulating rod (mm)	$57.2 \times 22.2 \times 642.0$
Absorber height (mm)	608.0
Absorber thickness (mm)	Control rod: 1.0; Regulating rod: 2.2
Cladding thickness in control rod	1.5 mm in each side of the absorber

2.2.2. Foils

The measurements were performed using activation foils, considering the activation reactions described in Table 2. Reaction rates (referred as foil responses) were determined after activity measurements using a HPGe detector.

Gold foils were used for thermal and epithermal neutron detection using the cadmium-ratio method (IAEA, 1970). The irradiation of foils, bare and covered by 1 mm-thick cadmium, allows discrimination between thermal and epithermal neutrons. Cadmium acts as a high-pass filter at approximately $E_{Cd} = 0.5$ eV (cadmium cut-off) which is the energy boundary between thermal and epithermal neutrons within this method. In the case of gold, a slight absorption of epithermal neutrons by the cadmium filter occurs, which is corrected by the factor $F_{Cd} = 1.008 \pm 0.9\%$ (Elnimr, 1990).

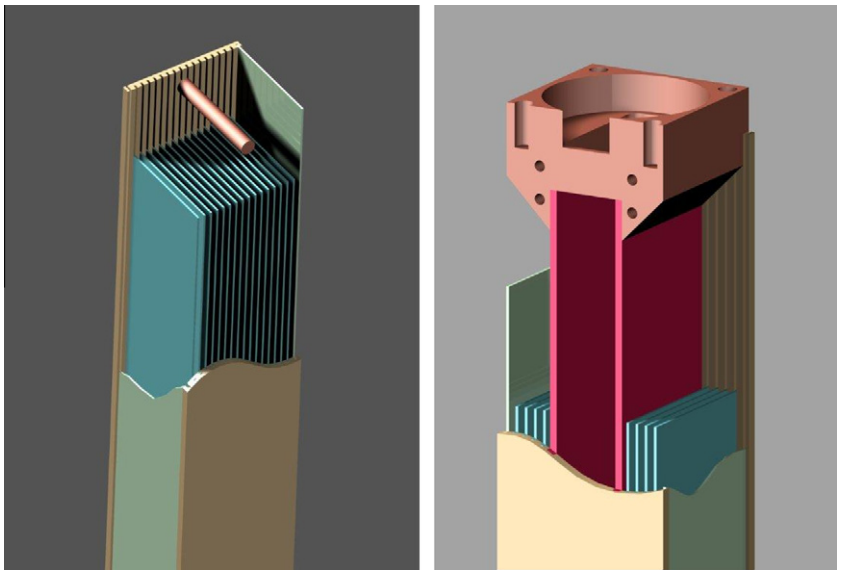

Fig. 2. Schematic view of fuel assemblies. Left: standard. Right: control.

Table 2
Activation foils and reactions used for neutron fluence rate measurements.

Reaction	Material and dimensions [a]	Reaction cross section [b]	Decay properties [c]
$^{197}Au(n,\gamma)^{198}Au$	Al–Au 0.1% w/w (∅5 × 0.1) mm Au (∅2 × 0.025) mm	σ_0 = 98.8(1) b I_r = 1570(3) b	$T_{1/2}$ = 2.656(3) d E_γ = 411.8 keV p_γ = 95.58%
$^{115}In(n,n')^{115m}In$	In (∅10 × 0.254) mm	σ_f = 184.8(31) mb	$T_{1/2}$ = 4.486(4) h E_γ = 336.2 keV p_γ = 45.8(22)%
$^{58}Ni(n,p)^{58}Co$	Ni (∅10 × 0.05) mm	σ_f = 105.5(18) mb	$T_{1/2}$ = 70.86(6) d E_γ = 810.7 keV p_γ = 99.450(10)%
$^{27}Al(n,\alpha)^{24}Na$	Al (∅10 × 0.125) mm	σ_f = 0.6860(93) mb	$T_{1/2}$ = 14.997(12) h E_γ = 411.8 keV p_γ = 99.9936(15)%

[a] ∅: diameter; w/w: weight fraction.
[b] σ_0: thermal cross section (at 25.3 meV); I_r: resonance integral; σ_f: fission-equivalent cross section (in ^{235}U fission spectrum).
[c] $T_{1/2}$: half-life of reaction product; E_γ and p_γ: energy and emission probability of the photons detected for activity measurements and detector response determination.

Certified Al–0,1%Au alloy (IRMM-530R, Institute for Reference Materials and Measurements, Belgium) was used in most positions in order to avoid self-shielding effects. For the measurements between plates in selected standard fuel assemblies, irradiations were performed at low reactor power, as the foil supports would block the cooling channel between the fuel plates, strongly restricting cooling by natural or forced convection. Thus pure gold foils were used, for which thermal and epithermal self-shielding factors are G_{th} = 0.964 ± 2% and G_{epi} = 0.362 ± 9%, respectively (Martinho et al., 2003).

Indium, Nickel and Aluminium foils (Goodfellow, UK) were used to characterize the fast region of the spectrum (neutron energy E > 1 MeV). Each foil set was wrapped in cadmium in order to reduce target and/or product burnup by thermal neutrons. In and Al foil activities were measured approximately 24 h after irradiation, while Ni was measured 3 days after irradiation to allow the decay of ^{58m}Co to ^{58}Co (half-life of 9.15 h).

2.2.3. Supports

The gold foils were mounted in polyethylene (PE) or polymethylmetacrylate (PMMA) rulers and distributed along the fuel length in order to obtain vertical fluence rate profiles. At standard fuel assemblies, distinct irradiations were performed for the bare and Cd-covered foils. For the remaining positions, bare and covered foils were placed in alternate positions along the ruler and irradiated together. The distance between the bare and covered foils was 5 cm in order to eliminate the influence of thermal flux depression by the Cd filters on adjacent foils (IAEA, 1970). Polynomial fittings (generally 3rd order polynomia) were applied to the measured response profiles of bare and covered foils in order to determine the corresponding responses at the same position.

Fast neutron measurements in the fuel assemblies were performed with sets of In, Ni and Al foils distributed in the PMMA rulers. For the remaining positions, a hollow cylindrical PE support with internal dimensions (∅4 × 16) cm was used, with foil sets placed in three positions along its axis, 7.5 cm apart. The influence of the support over the measurements due to the absence of water in its volume was calculated with MCNP. A simplified model was applied, considering a planar fission neutron source in water at 30 cm from the foil. Comparison of foil responses and fast neutron fluence rates calculated with a hollow and a water-filled support yielded a correction factor of −6% to measurements.

2.2.4. Irradiations

Reactor power and irradiation time were defined in order to achieve proper foil activities. Measurements in the fuel assemblies were performed at 100 W (Au) and 1 kW (In, Ni, Al) for 1–3 h, while measurements at the other positions were performed at 10–1000 kW for 1–12 h.

In general, reactor power was monitored using a pressurized argon ionisation chamber (50316, LND, USA) that measures the activity of ^{16}N in the primary cooling system (IAEA, 1997). This system lacked sensitivity for reactor power below 10 kW, in which case an ionisation chamber (CRGA, Compelec, France) placed at fuel mid-height in grid position 55 was used. Monitor responses were compared in the range 10–1000 kW in order to derive a power sensitivity factor for the CRGA chamber.

The monitoring signal was sampled during foil irradiations, once steady-state power level was achieved. The average value was used to determine the actual reactor power. The estimated uncertainty in power monitoring is 4%.

2.3. Neutron fluence rates

The cadmium-ratio method is based on the assumption that the neutron spectrum is reasonably described by the juxtaposition of a thermal Maxwellian to a $1/E$ epithermal distribution at the cadmium cutoff energy. From the responses of bare and covered foils, values for the conventional thermal neutron fluence rate (ϕ_0) and epithermal neutron fluence rate per unit lethargy (θ) are determined. ϕ_0 represents a mono-energetic neutron field in which all thermal neutrons have the most probable velocity of a Maxwellian distribution at 293 K. For the purpose of comparison to MCNP results, it is convenient to derive the total thermal (ϕ_{th}) and epithermal fluence rate between energies E_1 and E_2 (ϕ_{epi}^{E1-E2}). Conversion is made using the expressions (IAEA, 1970).

$$\phi_{th}/\phi_0 = (4/\pi\, T_n/T_0)^{1/2} \quad (1)$$

$$\phi_{epi}^{E1-E2} = \theta \ln(E_2 - E_1) \quad (2)$$

where T_n is the temperature of the thermal neutron distribution. Neutron temperature can be significantly larger than the moderator's (T_0 = 293 K) in regions where intense neutron absorption occurs (e.g., in the vicinity of the fuel).

Deviations from the $1/E$ epithermal spectrum can be frequently expressed by a distribution of the type $1/E^{1+\alpha}$, where α is a non-zero parameter (IAEA, 1970). Typical values of α range from −0.050 to +0.050 in a MTR reactor (Dung et al., 2010).

Concerning fast neutrons, the fission-equivalent fluence rates measured with each of the three foils (In, Ni and Al) are generally different, reflecting deviations between the actual neutron spectrum and that of ^{235}U fission (represented by the Watt–Cranberg distribution). An in-house developed code (BETA) uses these differences to adjust a fission-like spectrum, calculate the average

reaction cross sections in the adjusted spectrum and determine the neutron fluence rate above 1 MeV, ϕ_f (Gonçalves, 1985).

2.4. Monte Carlo calculations

Fig. 3 shows the RPI model produced with MCNP. The criticality mode was used to calculate the effective multiplication factor, foil responses and neutron fluences (F4 tally) per neutron produced in the fuel. Absolute values of responses and fluence rates at steady-state reactor power were calculated using the conversion factor

$$1\ \mathrm{Js^{-1}/W} \times 1\ \mathrm{MeV}/1.602\ \mathrm{J} \times 1\ \mathrm{fission}/200\ \mathrm{MeV} \times P\ \mathrm{W} \times \nu\ \mathrm{neutron/fission}$$

where P is the reactor power in Watt and ν is the average number of neutrons produced per fission, calculated by MCNP.

Transport cross section libraries used were mostly LANL:T16 for fissile and ENDF-B/6.0 for other elements, provided in the MCNP software package. Thermal neutron scattering by atoms bounded in molecules or lattice was included for graphite, hydrogen in water and beryllium. A constant temperature of 300 K was considered for all the materials.

Foil responses (FM card) were calculated using the continuous-energy IRDF-2002 dosimetry library (IAEA, 2006) for the reactions in Table 2.

Fluence rates were calculated in the 0–0.5 eV, 0.5 eV–10 keV and 1 MeV–20 MeV energy intervals (see Section 3.1). Detailed neutron spectra were also determined in the BUGLE-80 group structure (Roussin, 1980), with additional equi-lethargy groups in the thermal region in order to estimate the neutron temperature.

Detection volumes for neutron fluence rate and foil response tallying were simulated as water cylinders with a diameter of 3 mm (in standard assemblies) and 10 mm (remaining positions), corresponding to the foils positioning uncertainty. Detailed vertical neutron fluence rate profiles were obtained using adjacent volumes 3 cm-length, along the fuel height. Foil responses, neutron fluence rates and spectra were tallied in segments of 15 cm length located immediately below the fuel mid-height, where the maximum value of the vertical fluence rate distribution is known to occur (see Section 3.2). Since detection volumes are not filled with the foil materials, calculated foil responses refer to infinitely-diluted materials thereby neglecting the important self-shielding effects in pure gold foils.

Control rods were modelled at the vertical positions in which in practice the reactor becomes critical. Safety rods were displaced 56% of the fuel height, and the regulating rod was assumed to be at 40%. In the latter case the significant variations that usually occur during the irradiation in order to maintain the power level are disregarded due to the low reactivity worth of the regulating rod (in the order of 30%).

The criticality mode calculation was performed in a 3-stage scheme in order to reduce correlations between particle stories. An initial source distribution with one source point in each fuel assembly was used to run approximately 50 cycles of 3000 particles. The source distribution obtained was used in a subsequent run of 200 cycles of 20,000 particles. The source distribution obtained was finally used in cycles of 100,000 particles, the number of cycles depending on the statistical accuracy to be obtained in the tallies. The running time for 1 million particles was in the order of 50 min on a Core-2-Duo, 2.80-GHz personal computer.

3. Results and discussion

3.1. Neutron energy spectrum

The neutron spectra (neutron fluence rate per unit lethargy) calculated in a standard fuel and a dummy assembly at 1 MW reactor power are represented in Fig. 4 and Fig. 5, respectively. For comparison, the analytical distributions (thermal Maxwellian at 293 K, epithermal $1/E$ and Watt–Cranberg) are also represented. For the thermal region the Maxwellians were normalized to the calculated distributions assuring that their maxima have the same value, although they may occur for different energy bins in case the temperatures differ significantly. The $1/E$ and Watt–Cranberg distributions were normalized to the calculated fluence rate at 5 eV and the integral fluence rate above 1 MeV, respectively.

The neutron temperature was estimated by comparison of the lower-energy tails of the thermal distributions, yielding values in the order of 373 K at the fuel assemblies and 293 K for dummies, free grid positions and beryllium reflectors, reflecting the thermal equilibrium with the moderator. The high value for the neutron temperature in the standard fuel assemblies is consistent with measurements performed by other authors in reactors of similar design (e.g., Lloret, 1963; Koyama and Matsushita, 1980). Once the adequate neutron temperatures are considered, the Maxwell-

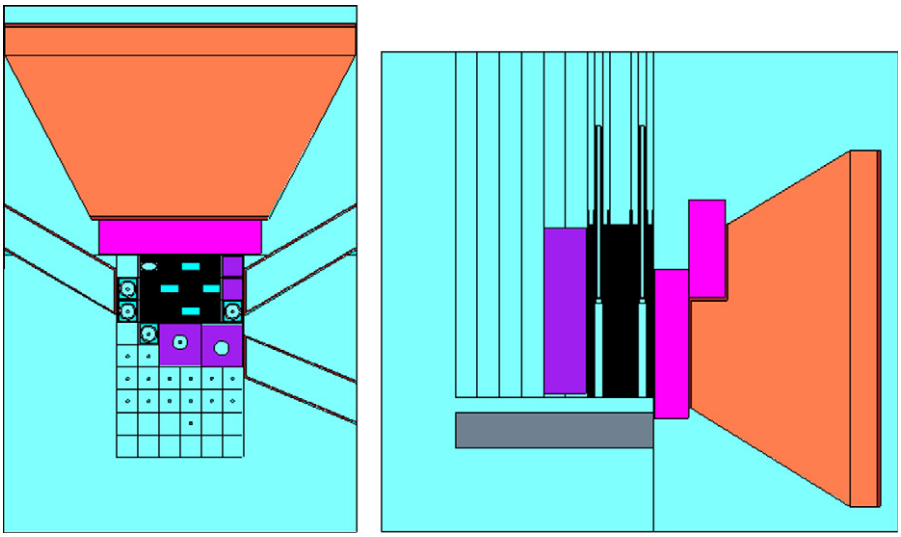

Fig. 3. MCNP model of the RPI core. Left: Horizontal cut-view, including the thermal column, beam tubes and detection volumes for neutron tallying. Right: Vertical cut-view, showing the grid plate and the displaced safety rods in control elements C2 and C3.

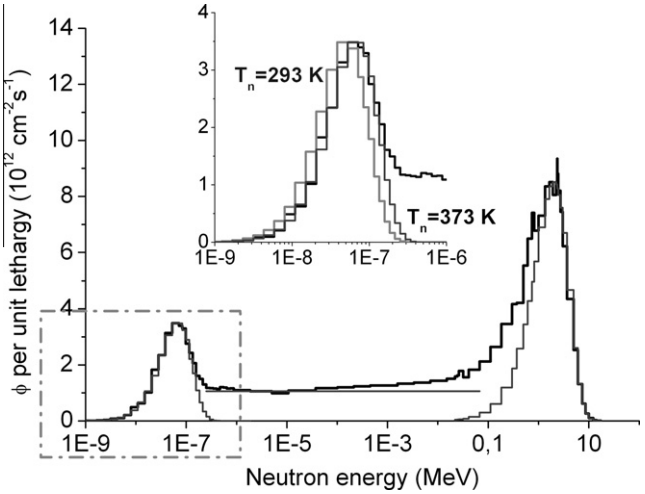

Fig. 4. Calculated spectra (black solid line) at 1 MW reactor power and adjusted analytical distributions (grey solid lines) at the standard fuel assembly S7, with a detailed view of the thermal energy region in order to exhibit the influence of the neutron temperature in the quality of the fitting.

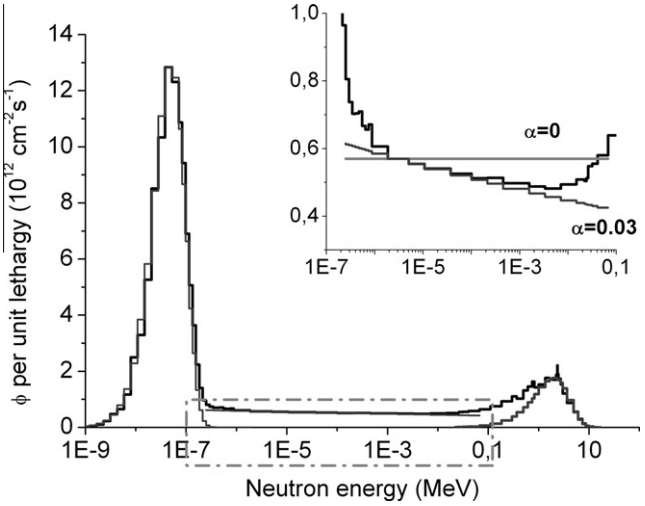

Fig. 5. Calculated spectra (black solid line) at 1 MW reactor power and adjusted analytical distributions (grey solid lines) at the dummy assembly in grid position 54, with a detailed view of the epithermal energy region in order to demonstrate the deviation from a $1/E$ distribution.

ian distribution describes very well the calculated spectra for energies up to 0.3–0.5 eV.

In the case of the epithermal distribution, a small deviation from the $1/E$ distribution was generally observed, with α in the order of 0.03–0.05 for most positions, except in the fuel assemblies. This analytical distribution is adequate to describe the energy spectrum in the energy interval from 1 eV to 1–10 keV.

At the fast energy region, a non-smooth structure is obtained between 500 keV and 2.5 MeV due to resonances in the elastic neutron scattering cross section in oxygen. Above this energy, the calculated spectrum is reasonably represented by the Watt–Cranberg distribution.

3.2. Distribution of neutron fluence rates along the fuel height

Fig. 6 shows measured and calculated relative thermal neutron fluence rate profiles along the fuel height, in a standard fuel assembly and a beryllium reflector. Uncertainties are smaller than 1%, and therefore not represented.

The calculated and measured profiles were normalized to the respective maxima, which occurs at 5–10 cm below the fuel mid-height due to the partial removal of the safety rods. In the case of the standard fuel assembly, simulated results exhibit a slight increase of the thermal neutron fluence rate at the lower end of the fuel due to the reflection by the core plate.

An excellent agreement (maximum deviation of 6%) between the relative profiles is achieved. This result differs considerable from that obtained in the previous MCNP models of the RPI using HEU fuel, in which deviations in the order of 20–30% were found at the lower half of the fuel, where burnup was more pronounced.

3.3. Foil responses

Table 3 shows the calculated average responses in a 15 cm segment below the fuel mid-height and their ratio to measured values. The normalisation factor for the MCNP tallies at 1 MW reactor power is 7.60E + 16.

The measured average responses of bare gold foils were determined after integrating the fitting polynomia in the referred region. For fast neutron foils, the arithmetic average of the three measurements was considered.

Uncertainties in measured data include the effect of reactor power monitoring (4%), activity measurements (2.5%, mostly from the efficiency calibration of the HPGe detector) and polynomial adjustments (1%), from which a combined value of 5% (1-sigma) is derived. For the calculated data, statistical uncertainties are indicated.

For the pure gold foils irradiated in the standard fuel assemblies, a multiplicative correction factor was applied to the measured foil responses, as the MCNP calculation neglected the self-shielding effect. In this region, the measured response ratio of bare to Cd-covered foils (cadmium-ratio, R_{Cd}) was approximately $R_{Cd} = 2{:}1$, which allows to derive a correction factor of $(1 - R_{Cd}^{-1})(G_{th}^{-1} + G_{epi}^{-1}) = 1.90 \pm 9\%$ (IAEA, 1970).

3.4. Neutron fluence rates

For comparison with measurements, thermal and epithermal neutron fluence rates were calculated in the energy intervals where the analytical distributions used in the formalism of the cadmium-ratio method are valid, i.e., from 0 to 0.5 eV (thermal) and 0.5 eV to 10 keV (epithermal). For fast neutron fluence rates the lower-energy limit is 1 MeV, in order to compare with the results determined using the BETA code.

Table 4 shows the calculated and measured average neutron fluence rates in a 15 cm segment below the fuel mid-height.

Propagation of uncertainties in the measured responses and data constants yields uncertainties of 5% for ϕ_{th} and ϕ_{epi} measurements in all irradiation positions (except at the fuel assemblies) and ϕ_f in every position. Concerning thermal and epithermal fluence rate measurements at the fuel assemblies, uncertainties are 12% and 10%, respectively. In the first case, the 5% uncertainty in the independent measurements of bare and covered gold foil responses becomes particularly important as both have similar values. In the second situation, the uncertainty is significantly increased due to the application of the epithermal self-shielding factor with pure gold foils. It is important to note that these uncertainties do not include the deviations between the real and analytical spectra, which were reduced through the judicious selection of the energy intervals where a reasonable agreement is obtained.

The discrepancy between calculated and measured neutron fluence rates is generally smaller than 15% for thermal and fast neutrons. In the epithermal range, discrepancies are slightly larger, up to 20%, reflecting the deviations between the calculated spectra

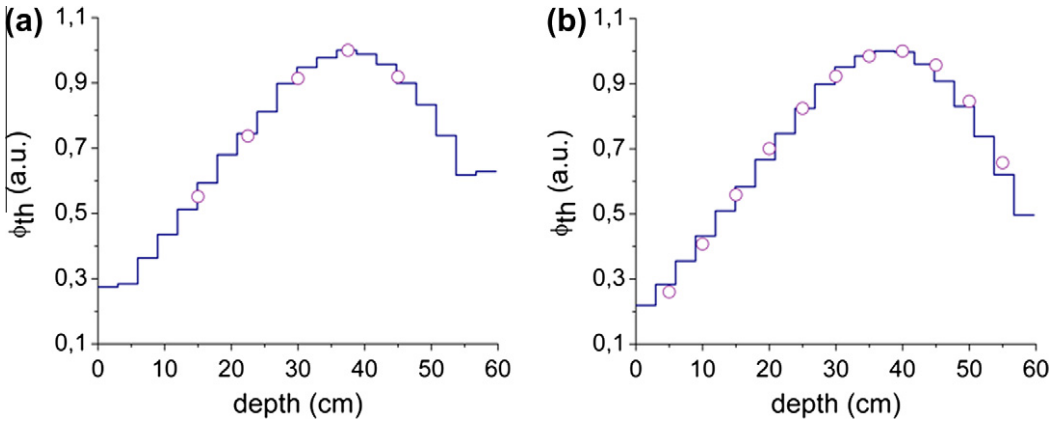

Fig. 6. Calculated (line) and measured (symbols) thermal fluence rate along the fuel height at (a) Standard fuel assembly S7; (b) Beryllium reflector Be–N. The fuel mid-plane is located at 30 cm depth.

Table 3
Calculated foil responses (C). The deviation from measured values (M) is indicated by the C/M ratio.

Position	Au		In		Ni		Al	
	C (10^{-11} s^{-1}) (%)	C/M	C (10^{-14} s^{-1}) (%)	C/M	C (10^{-14} s^{-1}) (%)	C/M	C (10^{-16} s^{-1}) (%)	C/M
Standard fuel assemblies								
S3	255 ± 2	1.03 ± 0.11	398 ± 0.4	1.06 ± 0.05	216 ± 0.5	0.95 ± 0.05	145 ± 3	1.14 ± 0.06
S7	212 ± 2	0.88 ± 0.09	324 ± 0.5	0.98 ± 0.05	178 ± 0.5	0.93 ± 0.05	119 ± 3	1.09 ± 0.06
S6	321 ± 2	1.02 ± 0.10	456 ± 0.4	1.00 ± 0.05	246 ± 0.5	0.90 ± 0.04	164 ± 2	1.06 ± 0.06
S5	270 ± 2	0.94 ± 0.10	387 ± 0.4	1.05 ± 0.05	205 ± 0.6	0.94 ± 0.05	131 ± 3	1.06 ± 0.06
Dummy fuel assemblies								
62	271 ± 0.6	1.05 ± 0.05	73.5 ± 0.5	1.01 ± 0.05	41.2 ± 0.6	0.92 ± 0.05	0.291 ± 3	1.05 ± 0.06
63	238 ± 0.7	1.11 ± 0.06	63.9 ± 0.5	0.93 ± 0.05	35.1 ± 0.6	0.95 ± 0.05	0.259 ± 3	1.07 ± 0.06
13	330 ± 0.6	1.10 ± 0.06	73.4 ± 0.5	1.06 ± 0.05	39.2 ± 0.6	0.96 ± 0.05	0.284 ± 3	1.12 ± 0.06
54	297 ± 0.6	1.05 ± 0.05	67.7 ± 0.5	0.90 ± 0.05	37.1 ± 0.6	0.81 ± 0.04	0.275 ± 3	0.98 ± 0.06
Beryllium reflector								
Be–N	372 ± 0.6	0.97 ± 0.05	50.0 ± 6	0.96 ± 0.05	25.0 ± 0.8	0.80 ± 0.04	20.9 ± 3	1.13 ± 0.07
Free grid positions								
65	38.4 ± 1	0.81 ± 0.05	6.61 ± 1	0.84 ± 0.04	4.29 ± 2	0.80 ± 0.05	4.24 ± 7	1.00 ± 0.08
55	104 ± 0.9	1.00 ± 0.05	12.4 ± 0.9	0.92 ± 0.05	7.23 ± 1	0.87 ± 0.05	6.57 ± 6	1.08 ± 0.08
66	7.79 ± 2	0.90 ± 0.05	1.62 ± 3	0.90 ± 0.05	1.15 ± 4	0.87 ± 0.05	1.26 ± 12	0.97 ± 0.13
56	19.9 ± 2	0.89 ± 0.05	2.61 ± 2	0.96 ± 0.05	1.72 ± 3	0.89 ± 0.05	1.88 ± 11	1.06 ± 0.12
46	40.9 ± 1	1.13 ± 0.06	2.91 ± 2	0.96 ± 0.05	1.74 ± 3	0.92 ± 0.05	1.71 ± 11	1.11 ± 0.13
36	49.0 ± 1	0.96 ± 0.05	3.09 ± 2	1.13 ± 0.06	1.81 ± 3	1.07 ± 0.06	1.99 ± 10	1.22 ± 0.14
26	41.2 ± 1	1.14 ± 0.06	2.37 ± 2	0.86 ± 0.05	1.35 ± 3	0.80 ± 0.05	1.34 ± 12	0.95 ± 0.13
16	24.0 ± 1	1.18 ± 0.06	1.42 ± 3	0.85 ± 0.05	0.840 ± 4	0.83 ± 0.05	1.21 ± 14	1.28 ± 0.19
67	1.93 ± 6	1.21 ± 0.09	0.432 ± 5	0.85 ± 0.06	0.334 ± 7	0.80 ± 0.07	0.410 ± 23	0.90 ± 0.21
57	3.15 ± 4	0.91 ± 0.06	0.552 ± 4	0.87 ± 0.07	0.393 ± 6	0.79 ± 0.06	0.527 ± 18	0.96 ± 0.18
47	4.53 ± 3	1.02 ± 0.06	0.639 ± 4	1.06 ± 0.07	0.467 ± 6	1.02 ± 0.08	0.537 ± 18	1.08 ± 0.20
37	4.91 ± 2	0.83 ± 0.04	0.626 ± 4	0.96 ± 0.06	0.451 ± 6	0.91 ± 0.07	0.375 ± 21	0.92 ± 0.15
27	4.30 ± 3	1.25 ± 0.08	0.514 ± 4	0.92 ± 0.06	0.368 ± 6	0.88 ± 0.07	0.371 ± 22	0.86 ± 0.19
17	2.54 ± 3	1.14 ± 0.07	0.347 ± 5	0.98 ± 0.07	0.275 ± 8	0.96 ± 0.09	0.408 ± 21	1.28 ± 0.28
38	0.672 ± 5	1.05 ± 0.08	0.168 ± 8	1.04 ± 0.10	0.146 ± 10	1.07 ± 0.12	0.230 ± 30	1.31 ± 0.39

and the $1/E$ distribution assumed in the cadmium-ratio formalism (as demonstrated in Figs. 4 and 5).

4. Conclusions

The MCNP code was used to determine thermal, epithermal and fast neutron fluence rates in the vicinity of the new RPI core using fresh LEU fuel. The calculations were compared with measurements performed with activation foils. An excellent agreement (within 6%) was obtained for the relative vertical fluence rate profiles along the fuel height. For the vertical displacement of safety rods leading to reactor criticality, the maximum fluence rate occurs at 5–10 cm below the fuel mid-height. Considering average values at the 15 cm segment below the fuel mid-height, the agreement between calculated and measured foil responses and neutron fluence rates was within 15% and 20%, respectively. In the second case, the achievement of such a good agreement required auxiliary calculations of the neutron spectrum, allowing the determination of neutron temperatures in the fuel region and the evaluation of energy intervals where the assumptions implicit in the activation method are valid.

In comparison with previous simulations of the RPI core using HEU fuel at high burnup values, the present work has demonstrated the capability of MCNP to determine autonomously the absolute values of neutron fluence rates, i.e., scaled for a specific reactor power and calculate accurately the vertical profiles of neutron fluence rate.

Concerning the experimental set-up, it is considered that the conditions applied did not lead to the best measurement accuracy, namely the application of hollow supports for fast neutron measurements and pure gold foils for thermal and epithermal neutron

Table 4
Calculated neutron fluence rates (C). The deviation from measured values (M) is indicated by the C/M ratio.

Position	ϕ_{th}		$\phi_{epi}^{0.5\ eV-10\ keV}$		ϕ_f	
	C (10^{12} cm^{-2} s^{-1}) (%)	C/M	C (10^{11} cm^{-2} s^{-1}) (%)	C/M	C (10^{11} cm^{-2} s^{-1}) (%)	C/M
Standard fuel assemblies						
S3	8.71 ± 0.5	1.00 ± 0.12	147 ± 0.4	1.29 ± 0.10	150 ± 0.3	1.08 ± 0.05
S7	7.87 ± 0.5	0.88 ± 0.12	117 ± 0.5	1.13 ± 0.10	123 ± 0.4	1.00 ± 0.05
S6	11.3 ± 0.4	1.15 ± 0.12	183 ± 0.4	1.15 ± 0.10	174 ± 0.3	1.05 ± 0.05
S5	9.92 ± 0.4	1.05 ± 0.12	151 ± 0.4	1.09 ± 0.10	147 ± 0.3	1.08 ± 0.05
Dummy fuel assemblies						
62	22.8 ± 0.2	1.12 ± 0.05	50.4 ± 0.4	1.05 ± 0.05	27.6 ± 0.4	1.03 ± 0.05
63	19.9 ± 0.2	1.16 ± 0.05	43.7 ± 0.4	1.10 ± 0.05	23.6 ± 0.4	0.89 ± 0.05
13	27.5 ± 0.2	1.18 ± 0.05	61.4 ± 0.4	1.03 ± 0.05	27.9 ± 0.4	1.09 ± 0.05
54	25.0 ± 0.2	1.12 ± 0.05	53.0 ± 0.4	0.99 ± 0.05	25.6 ± 0.4	0.92 ± 0.05
Beryllium reflector						
Be–N	31.3 ± 0.2	1.12 ± 0.05	65.8 ± 0.4	0.78 ± 0.05	19.8 ± 0.5	1.02 ± 0.05
Free grid positions						
65	3.89 ± 0.5	0.84 ± 0.05	3.48 ± 2	0.75 ± 0.05	2.55 ± 1	0.85 ± 0.05
55	10.2 ± 0.3	1.04 ± 0.05	9.59 ± 0.9	0.86 ± 0.05	4.94 ± 0.9	0.94 ± 0.05
66	0.828 ± 1	0.96 ± 0.06	0.732 ± 3	1.06 ± 0.06	0.612 ± 3	0.89 ± 0.06
56	2.05 ± 0.6	0.91 ± 0.06	1.40 ± 2	0.81 ± 0.06	1.01 ± 2	0.96 ± 0.05
46	4.22 ± 0.4	1.17 ± 0.05	2.69 ± 2	0.97 ± 0.05	1.19 ± 2	1.00 ± 0.05
36	5.00 ± 0.4	0.99 ± 0.05	3.12 ± 2	0.77 ± 0.05	1.27 ± 2	1.17 ± 0.05
26	4.26 ± 0.4	1.17 ± 0.05	2.57 ± 2	0.95 ± 0.05	0.989 ± 2	0.90 ± 0.05
16	2.55 ± 0.5	1.23 ± 0.06	1.35 ± 2	1.00 ± 0.06	0.588 ± 3	0.88 ± 0.06
67	0.177 ± 2	1.15 ± 0.09	0.156 ± 7	1.03 ± 0.09	0.162 ± 5	0.86 ± 0.07
57	0.313 ± 2	0.90 ± 0.08	0.232 ± 6	0.87 ± 0.08	0.214 ± 4	0.90 ± 0.07
47	0.469 ± 1	1.05 ± 0.07	0.294 ± 5	0.95 ± 0.07	0.243 ± 4	1.06 ± 0.06
37	0.529 ± 1	0.88 ± 0.07	0.339 ± 5	0.88 ± 0.07	0.244 ± 4	0.98 ± 0.06
27	0.443 ± 1	1.27 ± 0.07	0.250 ± 6	1.12 ± 0.07	0.201 ± 4	0.94 ± 0.07
17	0.271 ± 2	1.20 ± 0.08	0.158 ± 7	1.08 ± 0.08	0.134 ± 5	1.01 ± 0.07
38	0.0738 ± 3	1.16 ± 0.12	0.0720 ± 11	1.35 ± 0.12	0.0618 ± 8	1.03 ± 0.09

measurements. The independent irradiation of bare and covered gold foils in the fuel assemblies has significantly increased the measurement uncertainty and should be abandoned in favour of the application of bare and covered foils in alternate positions. For further uncertainty reduction, a different power monitoring system is being implemented conferring higher detection sensitivity and the ability to perform integrated measurements during foil irradiations.

Acknowledgements

The authors gratefully acknowledge Dr. J.G. Stevens from Argonne National Laboratory for his assistance in the early stages of this work.

References

Barradas, N.P., Cardeira, F., Fernandes, A.C., Gonçalves, J.G., Ramalho, A.J.G., 2000. Neutronics Study of Core 2 of the Portuguese Research Reactor. ITN/RPI-R-00/57, Instituto Tecnológico e Nuclear.

Briesmeister, J.F., 2000. MCNP-A general Monte Carlo N-Particle Transport Code System, Version 4C. LA-13709-M, Los Alamos National Laboratory.

Dung, M.H, Freitas, M.C., Santos, J.P., Marques, J.G., 2010. Re-characterization of irradiation facilities for k0-NAA at RPI after conversion to LEU fuel and re-arrangement of core configuration. Nuclear Instruments and Methods in Physics Research Section A. doi:10.1016/j.nima.2010.02.057.

Elnimr, T., 1990. Improved measurements of the correction factors for Cd shielding on neutron monitoring foils. Journal of Physics. D. Applied Physics 23, 1278–1281.

Fernandes, A.C., Gonçalves, I.C., Barradas, N.P., Ramalho, A.J., 2003. Monte Carlo modeling of the Portuguese Research Reactor core and comparison with experimental measurements. Nuclear Technology 143, 358–363.

Fernandes, A.C., Goncalves, I.C., Santos, J., Cardoso, J., Santos, L., Ferro Carvalho, A., Marques, J.G., Kling, A., Ramalho, A.J.G., Osvay, M., 2006. Dosimetry at the Portuguese Research Reactor using thermoluminescence measurements and Monte Carlo calculations. Radiation Protection Dosimetry 120, 349–353.

Gonçalves, I.C., 1985. Determination of the fast-neutron flux using the spectral indexes method. Atomkernenergie-kerntechnik 46, 212–213.

International Atomic Energy Agency, 1970. Neutron Fluence Measurements. IAEA Technical Report Series 107.

International Atomic Energy Agency, 1997. Research Reactor Instrumentation and Control Technology. IAEA TECDOC-973.

International Atomic Energy Agency, 2006. International Reactor Dosimetry File 2002 (IRDF-2002). IAEA Technical Report Series 452.

Koyama, M., Matsushita, M., 1980. Use of neutron spectrum sensitive monitors for instrumental neutron activation analysis. Bulletin of the Institute for Chemical Research, Kyoto University 58, 235–243.

Lloret, R., 1963. Mesure de la temperature du spectre des neutrons thermiques dans le coeur et le reflecteur de MELUSINE II. INT/Pi-171-150, Comissariat à l'Énergie Atomique CEA-CEN-G, Cadarache.

Martinho, E.M., Gonçalves, I.F., Salgado, J., 2003. Universal curve of epithermal neutron resonance self-shielding factors in foils, wires and spheres. Applied Radiation and Isotopes 58, 371–375.

Matos, J.E., Stevens, J.G., Feldman, E.E., Stillman, J.A., Dunn, F.E., Kalimullah, K., Marques, J.G., Barradas, N.P. Ramos, A.R., Kling, A., 2006. Core conversion analyses for the Portuguese Research Reactor. In: Proceedings of 28th International Meeting on Reduced Enrichment for Research and Test Reactors, South Africa. http://www.rertr.anl.gov/ (accessed 01.02.2010).

Roussin, R.W., 1980. BUGLE-80 Coupled 47-Neutron, 20-Gamma-Ray P3 Cross Section Library. DLC-75, Radiation Shielding Information Center. Oak Ridge National Laboratory.